Journal of Applied Polymer Science

Microscopic, structural, and electrical characterization of the carbonaceous materials synthesized from various lignin feedstocks

Singaravelu Vivekanandhan,[1,2]* Manjusri Misra,[1,2] Amar Kumar Mohanty[1,2]
Department of Plant Agriculture, Bioproducts Discovery and Development Centre, Crop Science Building, University of Guelph, Guelph, Ontario N1G 2W1, Canada
School of Engineering, Thornbrough Building, University of Guelph, Guelph, Ontario N1G 2W1, Canada
*Present address: Department of Physics, VHNSN College, Virudhunagar 626001, Tamilnadu, India
Correspondence to: M. Misra (E-mail: mmisra@uoguelph.ca)

ABSTRACT: Microscopic, structural and electrical characterization of the carbonaceous materials synthesized from different types of lignin precursors are investigated employing scanning electron microcopy (SEM), Raman spectroscopy, X-ray diffraction, and AC conductivity techniques. Lignin precursors from various resources carbonized at 900°C for 6 h under nitrogen atmosphere are used for this study. SEM analysis indicates formation of various microstructures, which are highly influenced by the carbonization behavior of lignin feedstocks that varies with chemical composition as well as purity. Raman spectroscopy of the carbon materials shows significant variations of its features, which represents their unique carbonization behaviors and graphitization events. Clear understanding of peak intensity, shape, and area gave very different structural features influenced by their chemical environment of the chosen precursor lignins. Phase purity and the graphitization degree are investigated through their X-ray diffraction patterns. © 2014 Wiley Periodicals, Inc. J. Appl. Polym. Sci. **2015**, *132*, 41786.

KEYWORDS: biopolymers and renewable polymers; microscopy; spectroscopy; synthesis and processing; X-ray

Received 21 April 2014; accepted 3 November 2014
DOI: 10.1002/app.41786

INTRODUCTION

Carbonaceous materials with various dimensional as well as structural features receives immense attention due to their scientific, technological, and commercial importance.[1,2] Carbon materials are highly diversified and normally found in a variety of product ranges including (i) micro and macro: carbon blacks, continuous, and chopped carbon fibers, fiber mats, activated carbon, carbon foams, and spheres and (ii) nano: fullerene, carbon nanotubes, graphenes, carbon nanofibers, nanoparticles, nano porous carbons, and carbon nanoonions.[3–5] Based on their different physicochemical properties they are used in many applications, such as electrochemical energy storage as well as conversion, catalysis, polymer and ceramic composites, filtrations, electronics, sensors, and medicine.[6–11] They have been synthesized from different types of carbon rich precursors by employing various processing techniques depending on the desired final products. A few examples of the precursor materials used in the fabrication of these carbon materials are acetylene, coal, pitch, poly (acrylonitrile), and rayon, which are basically petroleum resource based.[12–15] As the global concern regarding petroleum products rises, because of the ever-increasing crude oil price, nonrenewable nature of fossil fuel, and the increasing green house gas emission, there is a driven force to explore the sustainable alternative resources that offer environmental friendlyness and renewable origin for the fabrication of various carbon materials.

As a result, agro and forestry products including their biomass (wood, seeds, and fibers),[16–18] biomaterials, chemicals [cellulose, starch furfuryl alcohol (FA) and chitosan],[19–22] oil (palm oil),[23] and other kind of industrial residues (lignin, distiller grains, algal biomass)[24–26] have been widely investigated for the synthesis of various types of carbon materials. The practical challenges for the biobased feedstocks as the precursor for carbon materials are their lower yield during carbonization and difficulties in tailoring the properties of final products. Among the various bio feedstocks, lignin is found to be one of the efficient and versatile precursor for the fabrication of carbonaceous materials due to their carbon rich phenolic structure, abundance in nature and compatibility with various chemicals and polymers.[27,28] Next to cellulose, lignin is the second most available natural polymer, which exists approximately 30% by weight in plants.[29] They have been produced from

This article was published online on 24 Dec 2014. An error was subsequently identified. This notice is included in the online and print versions to indicate that both have been corrected 10 Jan 2015.

pulp and lignocellulosic biofuel industries as coproducts and need proper disposal due to the environmental issues. In order to enhance the economic viability, the biorefineries adopts a multiproduct strategy that explores the effective utilization of biomass as the feedstock for biochemicals and energy in addition to fuel. This increases the growth of lignocellulosic biorefineries that influences the lignin production significantly and tends to grow further. In general, lignin has been used as a low cost fuel and also to some extent in polymer blends and composites. In addition to that lignin has been used for the synthesis of various types of carbon materials including activate carbon, carbon black and carbon fibers. Recent developments in lignin based carbon materials are the fabrication of electrospun carbon nanofibers and other carbon based particulate nanostructures for various technological applications.[27,30–39] However, the nanofabrication techniques have not been investigated to a great extent. The challenge is to establish a common protocol for the various types of lignin, since the chemical structure and their related properties are highly diversified. Chemical architechture of lignin depends on two major factors; their sources and their related isolation techniques. Also, it is necessary to understand their property and product corelationships to overcome various hurdles in synthetic techniques for the fabrication of various types of carbonaneous materials with desired morphological and physicochemical properties.

As an example, photochemical and electrical performances of the lignin derived carbon materials are highly dependent on their microscopic and structural features. This arises from the structure condensation and graphitization of the lignin precursors during the carbonization process. Chemical structure and their purity level of lignin precursors are the key factor, which controls the condensation as well as graphitization event precisely. Understanding these co relationships is very critical in order to establish a suitable protocol for the fabrication of structure controlled carbon materials. Recently, Sahoo *et al.*[40] reported the characterization of various types of industrial lignins and discussed their structural and thermal properties. However, to the best of our knowledge, no literature work is available for the comparison of carbonaceous materials obtained from various lignin feedstocks. Hence, present work demonstrates the influence of various types of lignin precursors on the microscopic and structural features of the carbon materials and reveals their co-relationships. A systematic scanning electron microscopic (SEM), Raman and X-ray diffraction (XRD) analysis was performed on the synthesized carbon materials and the obtained results were discussed as presented.

EXPERIMENTAL

Materials

Bioethanol lignin, which is known as a by-product of hydrolyzed solid obtained from pretreated fibers was procured from Mascoma Canada. Water-soluble sodium carbonate lignin with strong anionic charges, which is commercially termed as Polybind 300 was supplied by Northway Lignin Chemical, Canada. Protobind 2400, a byproduct of paper industry, was purchased from ALM Private Limited, Hoshiarpur, Punjab, India. PolyFon O and Indulin lignin samples were procured from MeadWestvaco Corporation.

Lignin Carbonization

Carbonization of the lignins was performed in a tubular furnace equipped with air tightened alumina tube for the possible creation of various gas environments and it is schematically shown in Figure 1. The calculated amount of lignin samples (5 g) was filled in a sintered alumina boat and placed carefully into alumina tube. Both ends were closed and connected to the purge gas. In the present study, nitrogen gas was used to create an inert environment for the carbonization of lignin samples. Furthermore, the furnace was heated to 900°C (carbonization temperature) at the heating rate of 5°C per min and kept for 6 h to allow for carbonization followed by cooling of the room temperature at a cooling rate of 5°C per min. The synthesized carbonaceous materials were collected for further characterization.

Characterization

The microscopic structures of the synthesized carbon materials from different lignin precursors were investigated using Nova^{TM} Nano SEM Scanning Electron Microscope (SEM). Prior to SEM analysis all the carbon samples were sputter coated with a gold layer for the creation of a conducting surface in order to enhance the quality of the images. The micrograph was recorded at 15 kV accelerating voltage of the electron beam at a uniform magnification of 200×. Raman spectra of the synthesized carbon materials were recorded with a Renishaw 1000 Raman microscope equipped with an argon ion laser. Lignin derived carbon samples were grinded into fine particles and spread on a glass slide for Raman analysis. The spectra were recorded between 500 and 2000 cm^{-1} with the resolution of 4 cm^{-1}. Raman intensity for the 900°C prepared carbon sample was calculated after baseline correction between 500 and 2000 cm^{-1}. X-ray diffraction patterns of the synthesized carbon materials from various lignin precursors were recorded using Rigaku Multiflex X-ray powder diffractometer equipped with Cu-Kα radiation. The diffraction patterns were recorded between 10 and 80° 2θ values at 2° per min. Electrical conductivity of the carbon materials synthesized from different lignin precursors were investigated at room temperature using Autolab PGSTAT302N frequency responds analyzer employing the frequency range of 1 Hz to 250 KHz and 20 mV applied potential. Prior to conductivity measurement all the carbon materials were ball milled employing identical conditions. Approximately, 2 g of carbon samples synthesized from lignin precursors were ball milled for 1 h at 100 rpm using four steel balls each weighs 100 g in a Restech planetary ball Mill model PM 100. Oven dried powder samples (0.2 g) were placed in a cylindrical sample holder with an inner diameter of 10 mm. The measurement was performed under constant applied pressure of 1 ton. Conductivity of the carbon powder was calculated by employing following formula:

$$\sigma = ra/l$$

where "r" is bulk resistance obtained from impedance data, "a" is the area corresponding to the inner diameter of sample holder, which is calculated too and "l" is the thickness of the sample under applied pressure.

RESULTS AND DISCUSSION

Carbonization yields of the lignin precursors were calculated as 35.01, 57.49, 28.04, 55.17, and 42.50%, respectively, for the

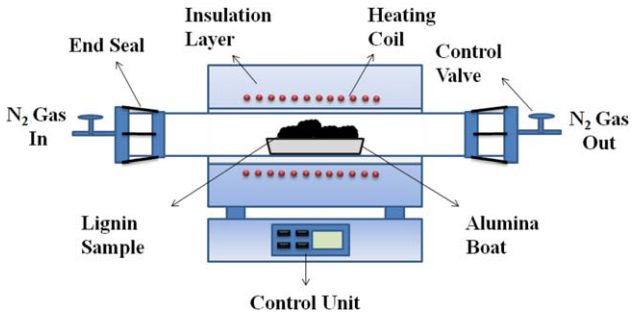

Figure 1. Schematic representation of the carbonization apparatus. [Color figure can be viewed in the online issue, which is available at wileyonlinelibrary.com.]

Bioethanol, Indulin, Polybind 300, PolyFon O, and Protobind 2400. A significantly lower yield was observed for the Polybind 300 lignin, which may be due to the presence of high moisture content (approximately 50%). In addition, Bioethanol results 35.01% carbonization yield, which indicates that the presence of cellulosic biomass lowers the yield. Physical appearance of the synthesized carbon materials from various types of lignin precursors are shown in Figure 2. The photographs illustrate that the carbon materials synthesized from bioethanol lignin results in dandified particulates, where as the carbon materials obtained from Indulin and PolyFon O lignins show light weight foamy structures. Other lignin's, Polybind 300, and Protobind 2400 resulted in the formation of flakey structures, in which carbon material obtained from Polybind exhibits soft and brittle in nature.

Scanning Electron Microscopy

SEM analysis of these carbon materials provides a clear understanding of their microscopic structure and the recorded micrographs at 200× magnification (uniformly to all samples) are shown in Figure 3. SEM micrograph of the carbon material synthesized from bioethanol lignin indicates the formation of solid lumps with more fibrous structures. The observed

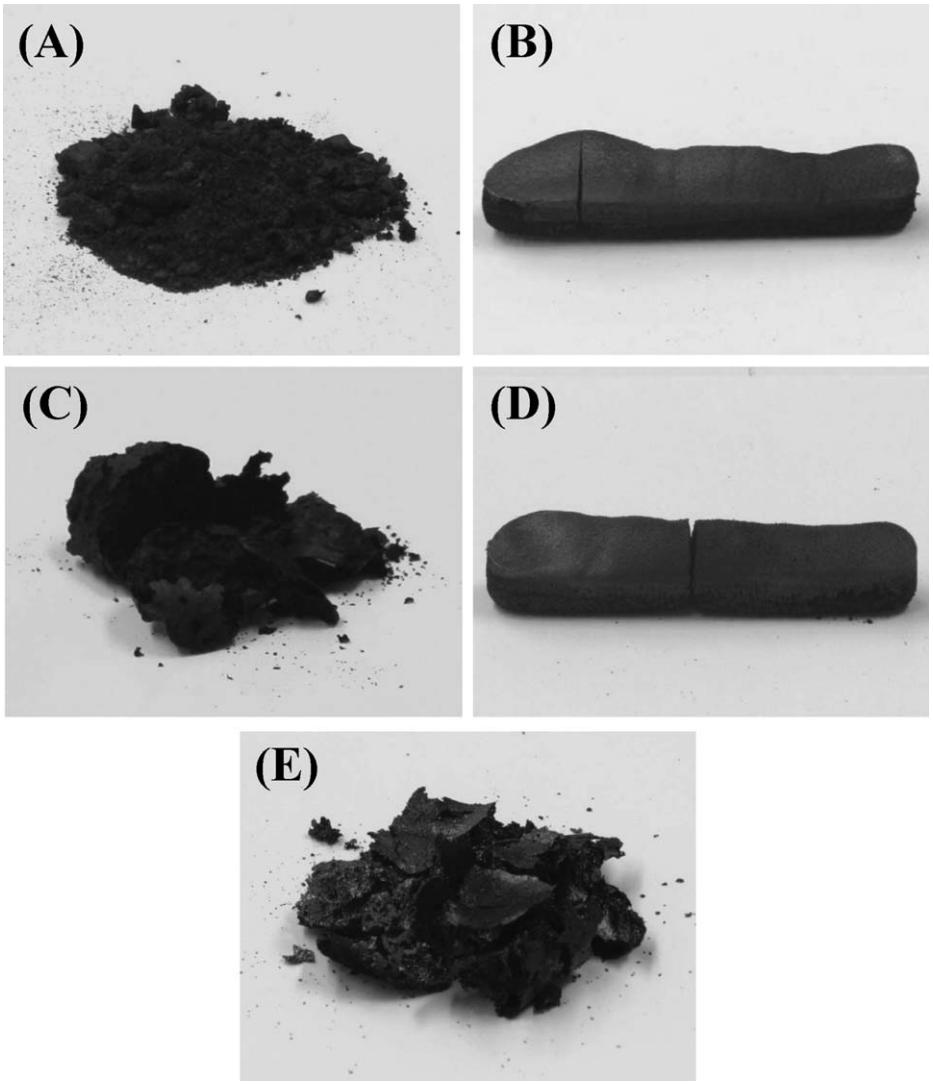

Figure 2. Photograph of the as synthesized carbon materials from various lignin precursors (A, bioethanol; B, Indulin; C, Polybind 300; D, PolyFon O; E, Protobind 2400).

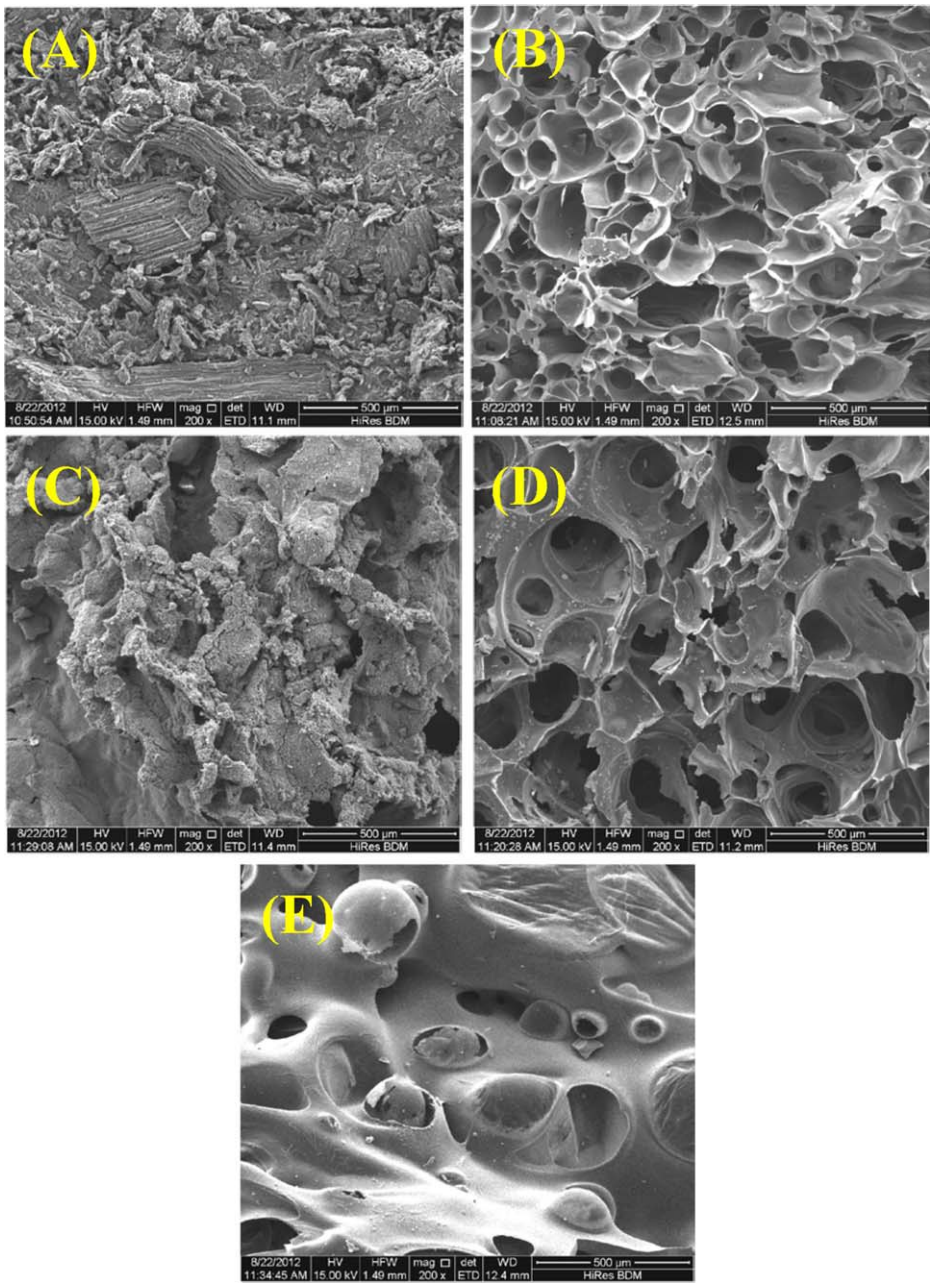

Figure 3. SEM micrograph of the carbon materials synthesized from various lignin precursors. (A, bioethanol; B, Indulin; C, Polybind 300; D, PolyFon O; E, Protobind 2400). [Color figure can be viewed in the online issue, which is available at wileyonlinelibrary.com.]

fibrous structures indicate the existence of significant amount of lingocellulosic biomass in the lignin precursor, which also remains in the carbonized materials. Comparing this observation with the carbon yield suggests that the existence of cellulosic biomass causes significant weight loss probably due to the presence of more oxygen in the cellulose structure, which oxidizes more carbon during the graphitization process. SEM micrographs of the obtained carbon materials from Indulin and PolyFon O clearly indicate the formation of a foamy structure. These macroporous networks consist of large amounts of pores and voids with a dimension range of 10–250 μm. The wall thickness of these foamy structures has been identified very thin and found to be few 100 nm. SEM micrograph of carbon materials obtained from Polybind lignin shows a solid lump structure and no significant feature is observed. However, the image indicates the random voids due to the evolved gases during the carbonization process. SEM image of the carbon materials synthesized from Protobind 2400 lignin shows a continuous flake like structure without any significant structural features; however it does show a lesser amount of voids.

Raman Spectroscopy

Raman spectroscopy is a simple and versatile technique in order to identify the structural features of carbon materials. Raman

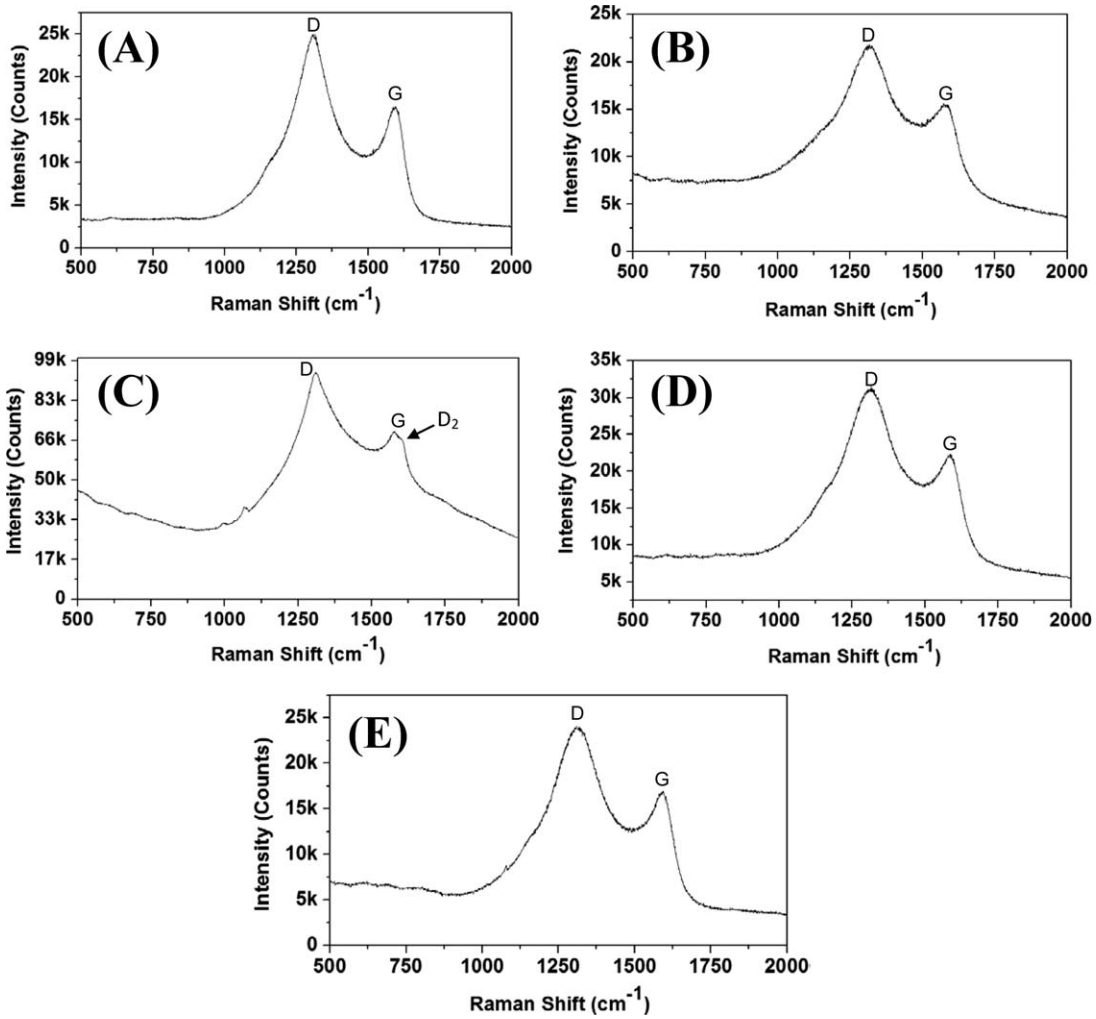

Figure 4. Raman spectra of the carbon materials synthesized from various lignin precursors. (A, bioethanol; B, Indulin; C, Polybind 300; D, PolyFon O; E, Protobind 2400).

spectra recorded for the synthesized carbon materials from various lignin precursors are shown in Figure 4. The obtained Raman spectra shows two distinguishable broad peaks at 1320 and 1580 cm^{-1} overlapped significantly. These two peaks were assigned to D and G bands, which are representing the characteristic peaks of the disordered and graphitic carbon archistructures, respectively.[41] For all the carbon materials, the D band (at 1320 cm^{-1}) intensities are observed to be higher than the G band (at 1580 cm^{-1}) which indicates the domination of disordered carbon structure related to the ordered graphite. This is significantly influenced by many key factors including source and chemical environment of the lignin precursors and also microstructure of the synthesized carbon. Intensity of both (D and G) the Raman peaks is also a critical parameter, which is proportional to the order of carbonization. In this point of view the carbon material synthesized from Polybind 300 lignin results in significantly higher intensity, which indicates the higher carbonization. Chemically Polybind 300 lignin consists of significant quantities of sodium, which promotes the graphitization and condensation behavior of lignin during the carbonization process and results in G band with higher intensities compared to the respective counterparts of other carbon materials. However, the domination of the D band still exists, which is due to the presence of sodium and related carbon structures.

Area Under the Peak. During the carbonization of lignin precursors at higher temperatures, the sp^3 carbons are condensed into the sp^2 carbons that exist in aromatic structures. Such structural change enhances their Raman scattering ability and results in higher Raman intensities. This reflects in their area under the curve as shown in Figure 5(a). In addition, the increased aromaticity of the carbon materials increases their light absorptivity, and decreases the Raman intensity. It has been suggested that the increasing light absorptivity dominate the light scattering ability of carbon materials effectively during the higher carbonization temperatures.[41] It can be understood that the varying total Raman intensities among the carbon materials is significantly influenced by their carbon skeletal structure, which may be caused by various chemical environments of the precursor lignins. In addition, the electron-rich structures, which are coupled with metallic clusters tends to show more Raman scattering behavior.[41] Thus, the carbon

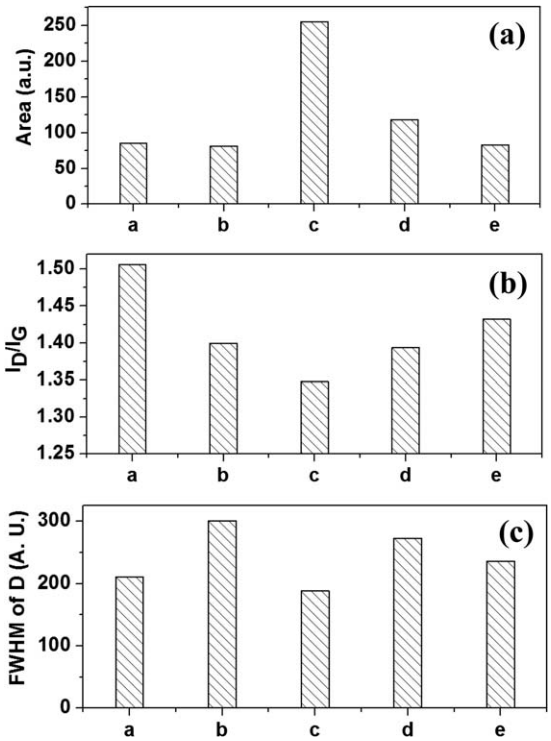

Figure 5. Total Raman peak areas (800–1800 cm^{-1}) (a), intensity ratios between bands D and G of the carbon materials (b), and FWHM of D band (c) of the carbon materials synthesized from various lignin precursors (A, bioethanol; B, Indulin; C, Polybind 300; D, PolyFon O; E, Protobind 2400).

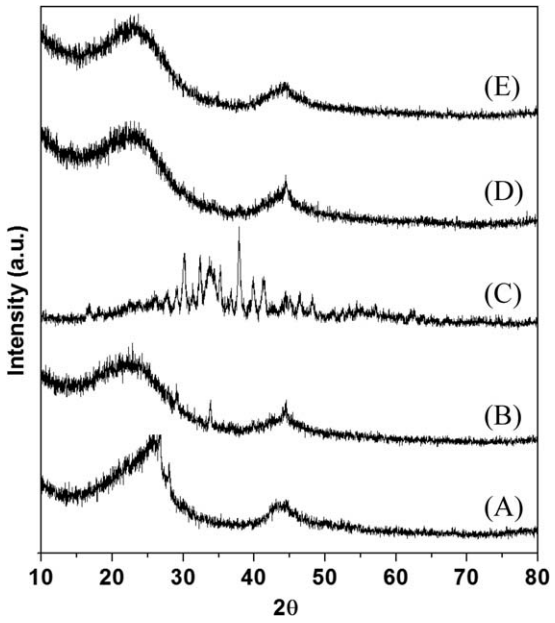

Figure 6. X-ray diffraction patterns of the carbon materials synthesized from various lignin precursors. (A, bioethanol; B, Indulin; C, Polybind 300; D, PolyFon O; E, Protobind 2400).

material synthesized from Polybind 300 lignin exhibits higher Raman intensity due to the presence of sodium metal.

Intensity Ratio of *D* and *G* Bands (I_D/I_G). Figure 5(b) shows the calculated intensity ratios of the *D* and *G* Raman bands of the synthesized carbon materials from various lignin precursors. As we defined earlier the *D* and *G* Raman bands are assigned to disordered defect and graphite like features of carbon respectively. Higher I_D/I_G ratio indicates the existence of a more disordered counterpart in the carbon sample. According to this, the highest I_D/I_G ratio was found in the carbon material synthesized from bioethanol lignin. Presence of momentous amounts of cellulosic counterpart in bioethanol lignin caused the inhibition of graphitization. During the carbonization process cellulosic materials that exist in the lignin precursor results in continued degradation, which inhibits the graphitization and results in more disordered carbon. Better condensation and graphitization were observed for the carbon material prepared from Polybind 300. Higher graphitization of Polybind 300 lignin compared to other lignin precursors is due to the presence of significant amounts of sodium (Na), which supports the graphitization during carbonization process. Metal enhanced graphitization mechanism was well understood by many researchers.[42–45]

Full-Width at Half-Maximum (FWHM). The graphitization order can be identified by calculating the full-width at half-maximum (FWHM) of the D band. Figure 5(c) shows the calculated FWHM of the synthesized carbon materials from various lignin precursors. Lowest FWHM was observed for the carbon material synthesized from Polybind 300, which indicates greater graphitization compared to other lignin precursors during the carbonization. Higher FWHM of D band was observed for the carbon materials synthesized from Indulin and PolyFon O lignin indicating the more disordered nature; which may be due to the formation of foamy microstructure. Enhanced graphitization of 300 Polybind lignin also supported by the presence of shoulder D2 band, which is not observed in the Raman spectra of other carbon materials.

X-ray Diffraction

X-ray diffraction analysis of carbon materials produced from various lignin precursors are shown in Figure 6. The obtained XRD pattern indicates the absence of well defined peak profiles except the carbon materials synthesized from Polybind300, which confirms the amorphous structure of carbon materials. The obtained nonindexed peak profiles for the carbon materials from Polybind300 are due to the presence of various metal related impurities. Being the sodium carbonate lignin Polybind300 has significant amount of sodium metal, which remains even after the carbonization. The XRD patterns of other carbon materials exhibits the two different broad profiles at 25° and 45° 2θ regions and they are assigned to the reflections form the (002) and (100/101) lines of graphitic sheets. XRD analysis has been extensively investigated for the determination of microstructures, which includes interlayer spacing (d) and crystallization size (L_C). In general d and L_C were calculated using the formula 1 and 2, respectively.

$$2\,d\,\sin(\theta) = n\lambda \quad (1)$$

Table I. Calculated d and L_C Values for the Carbon Materials Synthesized from Various Lignin Precursors

Source of the carbon material	2θ (°)	Interlayer distance, d (Å)	FWHM (°)	Crystallite size, L_C (Å)
Bioethonol	23.5	3.781	14.66	5.5
Indulin	21.3	4.166	18.96	4.2
Polybind	23.5	3.781	10.36	7.8
PolyFon	21.2	4.185	19.63	4.1
Protobind	21.7	4.090	18.41	4.3

$$L_C = (K\lambda)/\beta\cos(\theta) \quad \text{(Scherrer's formula)} \qquad (2)$$

where θ is the Bragg angle, λ-wavelength of the X-ray (1.54 Å), n-order parameter of the diffraction (normally 1), K is a Scherrer's constant (normally 0.9), β is the full-width half-maximum (FWHM) of the peak in radians. β and θ were obtained from Lorentz fit data. The calculated interlayer spacing (002) and the crystallite sizes are shown in Table I. These values were very much comparable with the published literature values for carbon black.[45] The lowest crystallite size was calculated (Å) for the carbon materials synthesized from PolyFon O lignin and the highest crystallite size was found to be Å for the carbon materials synthesized from Polybind 300. Lowest crystallite size for the carbon materials synthesized from Indulin, Poly Fon O, and Protobind 2400 are due to their foaming behavior, which inhibit the nucleation of carbon atoms during the carbonization process. This also caused the higher d spacing compared to the carbon materials synthesized from Polybind 300 and bioethanol lignins. The highest crystallite size for the carbon material obtained from Polybind 300 is due to the presence of sodium metal, which helps in increased condensing during the carbonization process.

Electrical Conductivity

Electrical conductivity of the carbonaceous materials that are synthesized from various lignin precursors is the cumulative effect of various factors that include particle size, surface area, contact among the individual particles, applied pressure, and the physicochemical nature of the carbon. The electrical behavior of the carbon powders were explained as Nyquist plot, which normally represent the complex impedance that integrates the real (Z') and imagery (Z'') as $Z^* = Z' \pm jZ''$. Figure 7(a) shows the Nyquist plot of the carbon materials synthesized from various lignin precursors. The plot indicates that the points are almost laid in a vertical line for all the carbon materials and the intersection of the plot at real axis indicates the bulk resistance. This value has been used to calculate the conductivity of the carbon materials and it is shown in Figure 7(b). Highest conductivity was observed for the carbon materials synthesized from Polybind300, which may be due to the presence of higher metal content. Lowest conductivity was observed for the carbon material obtained from bioethanol lignin, which may be due to the presence of significant amorphous counterpart. However, the electrical conductivity of the carbon materials synthesized from various lignin precursors depends on many factors and more investigation needs to be carried out to reveal their influence.

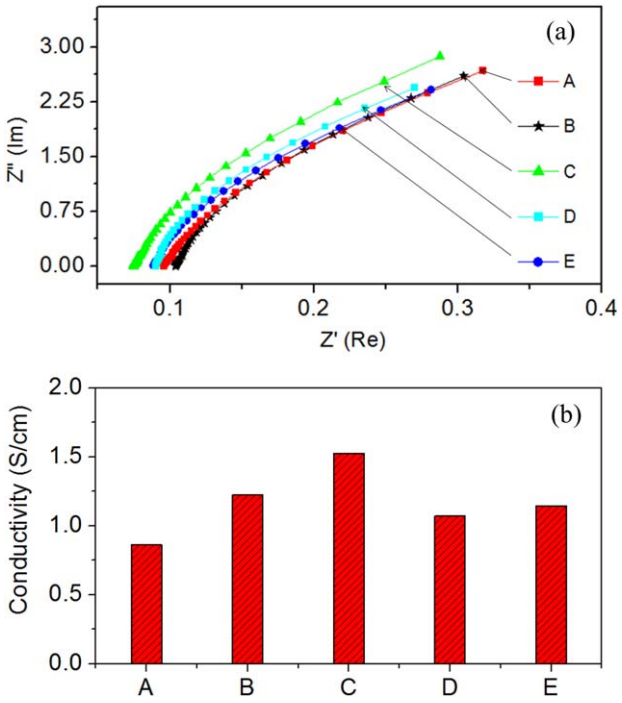

Figure 7. Nyquist plot (a) and electrical conductivity (b) of the carbon materials synthesized from various lignin precursors. (A, bioethanol; B, Indulin; C, Polybind 300; D, PolyFon O; E, Protobind 2400). [Color figure can be viewed in the online issue, which is available at wileyonlinelibrary.com.]

CONCLUSIONS

Microscopic and structural features of the carbon materials synthesized from various lignin feedstocks as carbon precursors were successfully investigated by employing SEM and Raman spectroscopic analysis. From this study we have revealed the relationship between physicochemical nature of the lignin precursors and their carbonization behavior. The key result of this study is summarized below:

- Lignin from the bioethanol industry shows significant amount cellulosic biomass, which lowers the yield of carbon product.
- Purity and the chemical environment of the lignin play a key issue in the carbonization process as well as graphitization mechanism.
- Carbon materials obtained from Indulin and PolyFon O lignins shows an excellent foamy microstructure and can be effectively used for the fabrication of various carbon monoliths with foamy architecture.
- Enhanced graphitization was observed for the Polybind 300 lignin compared to other lignin feedstocks, which is due to the presence of excess sodium metal.

- XRD analysis indicates that the carbon materials obtained from Indulin, PolyFon O, and Protobind 2400 resulted in the lowest graphite crystallize size.
- The highest crystallite size observed for the Polybind 300 lignin is due to the highest degree of condensation during the carbonization process, which was catalyzed by sodium ions.
- Existence of metals in lignin precursors influenced the electrical conductivity of their respective carbon product.

ACKNOWLEDGMENTS

The authors are thankful to the Ontario Ministry of Agriculture, Food and Rural Affairs (OMAFRA)—New Directions and Alternative Renewable Fuels Research Program; OMAFRA—University of Guelph Bioeconomy—Industrial uses Research Program; the Ministry of Economic Development and Innovation (MEDI), Ontario Research Fund—Research Excellence Round—4 program; the Natural Sciences and Engineering Research Council (NSERC), Canada for the Discovery grants individual (to Mohanty); and NSERC Networks of Centres of Excellence (NCE) AUTO21 project for the financial support to carry out this research work.

REFERENCES

1. Gogotsi, Y. Carbon Nanomaterials; Taylor and Francis: Boca Raton, **2006**.
2. Sheehan, J. E.; Buesking, K. W.; Sullivan, B. *J. Annu. Rev. Mater. Sci.* **1994**, *24*, 19.
3. Shenderova, O.; Zhirnov, V.; Brenner, D. *Crit. Rev. Solid State Mater. Sci.* **2002**, *27*, 227.
4. Choi, W.; Lahiri, I.; Seelaboyina, R.; Kang, Y. S. *Crit. Rev. Solid State Mater. Sci.* **2010**, *35*, 52.
5. Sinnott, S. B.; Andrews, R. *Crit. Rev. Solid State Mater. Sci.* **2001**, *26*, 145.
6. Frackowiak, E; Beguin, F. *Carbon* **2001**, *39*, 937.
7. Rodriguez-Reinoso, F. *Carbon* **1998**, *36*, 159.
8. Stankovich, S.; Dikin, D. A.; Dommett, G. H. B.; Kohlhaas, K. M.; Zimney, E. J.; Stach, E. A.; Piner, R. D.; Nguyen, S. T.; Ruoff, R. S. *Nature* **2006**, *442*, 282.
9. Li, H.; Gui, X.; Zhang, L.; Wang, S.; Ji, C.; Wei, J.; Wang, K.; Zhu, H.; Wu, D.; Cao, A. *Chem. Commun.* **2010**, *46*, 7966.
10. Takahashi, T.; Takei, K.; Gillies, A. G.; Fearing, R. S.; Javey, A. *Nano Lett.* **2011**, *11*, 5408.
11. Liu, Z.; Robinson, J. T.; Tabakman, S. M.; Yang, K.; Dai, H. *Mater. Today* **2011**, *14*, 316.
12. Li, W.; Long, D.; Miyawaki, J.; Qiao, W.; Ling, L.; Mochida, I.; Yoon, S. H. *J. Mater. Sci.* **2012**, *47*, 919.
13. Immanuel, V.; Meenakshi, K. S. *Indian J. Sci. Technol.* **2011**, *4*, 759.
14. Mao, L.; Tong, S.; Zhang, X.; Fan, M.; Wan, L.; Jia, C. Q. Preparation of Coal Tar Pitch Based Mesoporous Activated Carbon by Template and KOH Activation Method. Intelligent Computation Technology and Automation (ICICTA), 2011 International Conference on IEEE, pp 880–883.
15. Su, C. C.; Chang, S. H. *Mater. Lett.* **2011**, *65*, 1114.
16. Murr, L. E.; Guerrero, P. A. *Atmos. Sci. Lett.* **2006**, *7*, 93.
17. Sharon, M.; Soga, T.; Afre, R.; Sathiyamoorthy, D.; Dasgupta, K.; Bhardwaj, S.; Sharon, M.; Jaybhaye, S. *Int. J. Hydrogen Energy* **2007**, *32*, 4238.
18. Kang, Z.; Wang, E.; Mao, B.; Su, Z.; Chen, L.; Xu, L. *Nanotechnology* **2005**, *16*, 1192.
19. White, R. J.; Budarin, V.; Luque, R.; Clark, J. H.; Macquarrie, D. J. *Chem. Soc. Rev.* **2009**, *38*, 3401.
20. Jazaeri, E.; Zhang, L.; Wang, X.; Tsuzuki, T. *Cellulose* **2011**, *18*, 1481.
21. Bertarione, S.; Bonino, F.; Cesano, F.; Jain, S.; Zanetti, M.; Scarano, D.; Zecchina, A. *J. Phys. Chem. B* **2009**, *113*, 10571.
22. Bengisu, M.; Yilmaz, E. *Carbohydr. Polym.* **2002**, *50*, 165.
23. Suriani, A. B.; Azira, A. A.; Nik, S. F.; Md Nor, R.; Rusop, M. *Mater. Lett.* **2009**, *63*, 2704.
24. Kadla, J. F.; Kubo, S.; Venditti, R. A.; Gilbert, R. D.; Compere, A. L.; Griffith, W. *Carbon* **2002**, *40*, 2913.
25. Heilmann, S. M.; Jader, L. R.; Sadowsky, M. J.; Schendel, F. J.; VonKeitz, M. G.; Valentas, K. *J. Biomass Bioenergy* **2011**, *35*, 2526.
26. Yanik, J.; Stahl, R.; Troeger, N.; Sinag, A. *J. Anal. Appl. Pyrol.* **2013**, *103*, 134.
27. Ruiz-Rosas, R.; Bedia, J.; Lallave, M.; Loscertales, I. G.; Barrero, A.; Rodríguez-Mirasol, J; Cordero, T. *Carbon* **2010**, *48*, 696.
28. Babeł, K.; Jurewicz, K. *Carbon* **2008**, *46*, 1948.
29. Calvo-Flores, F. G.; Dobado, J. A. *ChemSusChem* **2010**, *3*, 1227.
30. Lallave, M.; Bedia, J.; Ruiz-Rosas, R.; Rodríguez-Mirasol, J.; Cordero, T.; Otero, J. C.; Marquez, M.; Barrero, A.; Loscertales, I. G. *Adv. Mater.* **2007**, *19*, 4292.
31. Dallmeyer, I.; Ko, F.; Kadla, J. F. *J. Wood Chem. Technol.* **2010**, *30*, 315.
32. Ago, M.; Okajima, K.; Jakes, J. E.; Park, S.; Rojas, O. J. *Biomacromolecules* **2012**, *13*, 918.
33. Schreiber, M.; Vivekanandhan, S.; Mohanty, A. K.; Misra, M. *Adv. Mat. Lett.* **2012**, *3*, 476.
34. Schreiber, M.; Vivekanandhan, S.; Cooke, P.; Mohanty, A. K.; Misra, M. *J. Mater. Sci.* **2014**, *49*, 7949.
35. Schreiber, M.; Vivekanandhan, S.; Mohanty, A. K.; Misra, A. C. S. *Sustain. Chem. Eng.* **2014**, Doi:10.1021/sc500481k.
36. Poursorkhabi, V.; Mohanty, A. K.; Misra, M. *J. Appl. Polym. Sci.* **2015**, *132*, 41260.
37. Snowdon, M. R.; Mohanty, A. K.; Misra, M. *ACS Sustain. Chem. Eng.* **2014**, *2*, 1257.
38. Gonugunta, P.; Vivekanandhan, S.; Mohanty, A. K.; Misra, M. *World J. Nano Sci. Eng.* **2012**, *2*, 148.
39. Gonugunta, P. Synthesis and Characterization of Biobased Carbon Nanoparticles from Lignin. Master Thesis, University of Guelph, **2012**.
40. Sahoo, S.; Seydibeyoğlu, M. Ö.; Mohanty, A. K.; Misra, M. *Biomass Bioenergy* **2011**, *35*, 4230.

41. Keown, D. M.; Li, X.; Hayashi, J. I.; Li, C. Z. *Energy Fuels* **2007**, *21*, 1816.
42. Weisweiler, W.; Subramanian, N.; Terwiesch, B. *Carbon* **1971**, *9*, 755.
43. Yudasaka, M.; Kikuchi, R. Graphitization of Carbonaceous Materials by Ni, Co and Fe. Yoshimura, S.; Chang, R. P. H. Eds.; Supercarbon; Springer: Heidelberg, **1998**, pp 99–105.
44. Kormann, M.; Gerhard, H.; Zollfrank, C.; Scheel, H.; Popovska, N. *Carbon* **2009**, *47*, 2344.
45. Borah, D.; Satokawa, S.; Kato, S.; Kojima, T. *Appl. Surf. Sci.* **2008**, *254*, 3049.